PCCP

Benzene⋯Acetylene: A structural investigation of the prototypical CH⋯π interaction

SCHOLARONE™
Manuscripts

Benzene···Acetylene: A structural investigation of the prototypical CH···π interaction

Nathan W. Ulrich,[a] Nathan A. Seifert,[b] Rachel E. Dorris,[a] Rebecca A. Peebles,[a] Brooks H. Pate,[b]

Sean A. Peebles [a, *]

[a] Eastern Illinois University, Department of Chemistry, 600 Lincoln Ave., Charleston, IL 61920

[b] University of Virginia, Department of Chemistry and Biochemistry, McCormick Rd., PO Box

400319, Charlottesville, VA 22904

*To whom correspondence should be addressed:

email: sapeebles@eiu.edu

phone: (217) 581-2679

Abstract

The structure of a prototype CH···π system, benzene···acetylene, has been determined in the gas phase using Fourier-transform microwave spectroscopy. The spectrum is consistent with an effective C_{6v} structure with an H···π distance of 2.4921(1) Å. The HCCH subunit likely tilts by ~5º from the benzene symmetry axis. The dipole moment was determined to be 0.438(11) D from Stark effect measurements. The observed intermolecular distance is longer than in similar benzene···HX complexes and than the distances observed in the benzene···HCCH cocrystal and predicted by many high level ab initio calculations; however, the experimentally estimated binding energy of 7.1(7) kJ mol^{-1} is similar to previously studied benzene···HX complexes. Several additional sets of transitions were observed in the rotational spectrum, likely corresponding to excited states arising from low energy intermolecular vibrational modes of the dimer.

Introduction

The dimer between benzene (BZ) and acetylene (HCCH) is a prototype system for the study of weak CH···π interactions, where the π electrons are part of an aromatic system. These interactions have been known for many years to be important in a wide range of chemical circumstances, and they were first noted as long ago as 1952, with Tamres's calorimetric measurements in solutions of chloroform with aromatic compounds.[1] Experimentally, most examples of aromatic CH···π interactions have been identified in crystal structures or by IR or NMR spectroscopy[2, 3, 4] (although some gas phase studies are also available[2, 3, 5-19]) with the most often studied interactions involving an alkyl hydrogen atom oriented towards the center of an aromatic ring.[20] Most spectroscopic investigations have not attained sufficient resolution to

obtain detailed structural information about the clusters,[4-9, 12, 15, 19] although high resolution

(rotational spectroscopy) studies of fluorobenzene···HCCH[18], BZ···HCF$_3$,[13, 14] and benzene

dimer[16, 17] are available. These provide structural information on the isolated weak CH···π

contact without the possible influence and constraints of crystal packing. In addition to the BZ

and fluorobenzene complexes listed above,[13, 14, 16-19] aromatic XH···π contacts to benzene have

been observed by gas phase rotational spectroscopy in the complexes of BZ with HBr,[21] HCl,[22]

HF,[23] HCN,[24] H$_2$S,[25] and H$_2$O,[26, 27] providing numerous examples of XH···π interactions with

which CH···π interactions may be compared.

BZ···HCCH provides an interesting intermediate step between typical CH···π interactions

with an alkyl hydrogen atom and the stronger XH···π interactions that have been the primary

focus of many previous microwave spectroscopic studies.[21-27] The hydrogen atoms of HCCH are

relatively acidic, with a pK_a of ~25,[28] so that the hydrogen atom of HCCH is activated compared

with an alkyl hydrogen atom. Thus, it is expected that the interaction between HCCH and BZ

may be stronger than the interactions observed in typical (not activated) CH···π complexes. This

has been confirmed by Shibasaki, *et al.* using two-color multiphoton ionization spectroscopy,

where it was shown that the binding energy of BZ···HCCH is significantly larger ($D_0 = 11(1)$ kJ

mol^{-1})[11] than that observed for BZ···CH$_4$ ($D_0 = 4.5(2)$ kJ mol^{-1}).[10] (By way of comparison,

fitting rotational spectroscopic data to an intermolecular potential gives $D_0 \approx 4.7$ kJ mol^{-1} for

BZ···Ar,[29] similar to the value for CH$_4$.) Binding energies of $D_0 \sim 6 - 22$ kJ mol^{-1} have been

observed for other activated CH donors such as chloroform and other haloalkanes.[6, 20, 30] López

used rotational spectroscopic results to estimate a binding energy for BZ···HCF$_3$[13] of 8.4 kJ

mol^{-1}, within a few kJ mol^{-1} of Shibasaki's value for BZ···HCCH.[11, 20] The similarity of pK_a

values for HCCH and HCF$_3$ might suggest that the two benzene complexes should be similar

energetically.[28, 31] Tsuzuki[20] also analyzed the nature of the noncovalent interactions in a series of benzene CH···π complexes and found that, while typical CH···π interactions are primarily driven by dispersion forces, activated CH···π interactions also have a significant electrostatic contribution. Although dispersion is still the largest contributor to the interaction energy for the activated complexes, the increased electrostatic contribution relative to typical CH···π interactions leads to stronger and more directional CH···π contacts. In addition, most CH···π interactions investigated by Tsuzuki displayed a small red-shift in the CH stretch frequency upon complexation, consistent with the expected low frequency shift upon formation of a, typically much stronger, hydrogen bonding interaction (and in contrast to "improper" CH···X interactions that typically exhibit a blue-shifted CH stretch).[20]

A large body of theoretical data consistently predicts that the most stable structure of BZ···HCCH will have HCCH aligned more or less along the C_6 axis of BZ, with a possible small tilt of the HCCH axis away from the BZ symmetry axis.[11, 30, 32-38] Estimates of the H···π distance range from 2.20 to 2.61 Å,[35, 36] with high level CCSD(T)/aug-cc-pVTZ calculations predicting a distance of ~2.50 Å.[35] Much recent theoretical work has focused on testing various density functional theory (DFT) methods for optimization and energy calculations of BZ···HCCH.[34, 37, 39] The best DFT results, as judged by comparison of interaction energies with estimated CCSD(T)/CBS calculations, have been obtained using the M05-2X, M06-2X and ωB97X-D functionals, with an M06-2X/6-311+G(d,p) calculation giving an H···π distance of 2.393 Å and a binding energy of 12.2 kJ mol^{-1}.[39] No previous gas-phase structure determinations exist; however, a BZ···HCCH cocrystal has been studied by X-ray diffraction.[40] That study confirms the alignment of HCCH along the benzene C_6 axis and gives an H···π distance of 2.447 Å at 123 K (and 2.462 Å at 201 K),[40] in reasonable agreement with the theoretical calculations. The

crystal structure also indicates that HCCH likely tilts away from an axis connecting adjacent BZ molecules by ~15 – 24º. Gas phase studies of BZ···HCCH utilizing UV spectroscopy have shown evidence of a second isomer for the dimer, consistent with a structure in which the HCCH axis is parallel to and above the BZ plane, aligned along a C–C bond of BZ, with the whole complex maintaining C_s symmetry;[5] however, no evidence was found in the co-crystal or the present study for the formation of this second structure. The only crystallographic evidence for a role reversal, with BZ acting as a proton donor to an acetylenic π acceptor, is of co-crystals of BZ with much larger substituted acetylenes in which the acidic acetylenic protons have been replaced by either trimethyl(silyl) groups or phenyl groups.[41] Microwave spectroscopic studies also show that in BZ dimer the BZ acts as both CH donor and acceptor, with the dimer taking on a T-shaped configuration.[16, 17]

In the present work we undertake a chirped-pulse Fourier-transform microwave (CP-FTMW) spectroscopic study of the BZ···HCCH complex, in order to precisely determine the gas-phase structure of the dimer, as well as making new experimental estimates of the binding energy and intermolecular stretching frequency. A predicted dipole moment of ~0.5 D indicates that the dimer is sufficiently polar to observe using the CP-FTMW spectrometer at the University of Virginia (UVa).[42, 43] It is hoped that these results will provide fundamental information for comparison with future computational studies of this prototype for aromatic CH···π interactions, as well as increasing the body of experimental data on these very weakly bound species.

Experimental

Chirped-pulse Fourier-transform microwave (CP-FTMW) spectroscopy was used to record the rotational spectrum of the BZ···HCCH weakly bound complex in the 6 – 20 GHz

range. The spectrum was recorded using the CP-FTMW spectrometer at the University of

Virginia (UVa). The instrument has been described elsewhere,[42, 43] so only relevant

experimental details are presented here. The sample consisted of 0.1% BZ (Aldrich) and 0.2%

HCCH (Praxair) diluted to about 1.7 atm total pressure with Ne. Five nozzles were fired

simultaneously, at a repetition rate of 3.3 Hz. For each gas pulse, 8 free induction decays (FID)

were recorded, each corresponding to excitation from a single 2 μs chirp broadcast into the

vacuum chamber. The final spectrum was an average of 520,000 FIDs, corresponding to a total

recording time of ~4.5 hours. In addition, a second broadband scan using a sample of C_6H_5D

(99%, Aldrich; 400,000 FIDs; 3.0 atm) was recorded to allow analysis of the $C_6H_5D\cdots$HCCH

spectrum. Finally, measurements of the two BZ$\cdots$ H^{13}C^{12}CH isotopologues were recorded using

an enriched sample (99.2% ^{13}C, CDN Isotopes) with the resonant cavity FTMW spectrometer at

Eastern Illinois University (EIU).[44, 45] For measurements made using the resonant cavity

instrument, the sample consisted of 0.5% each of BZ and H^{13}C^{12}CH diluted to a total pressure of

~2.8 atm in He/Ne. A single nozzle was aligned perpendicular to the direction of microwave

propagation, with a nozzle repetition rate of 10 Hz, and one FID recorded per gas pulse. The

cavity FTMW instrument was also used to measure Stark effects, leading to a dipole moment

determination for the BZ$\cdots$HCCH complex. For the Stark effect measurements, potentials of up

to ±5 kV were applied to a pair of parallel steel mesh plates, separated by ~31 cm and straddling

the Fabry-Perot cavity of the spectrometer. The electric field was aligned parallel to the

microwave antennas so only $\Delta M = 0$ Stark effects would be observed. The field was calibrated

using the $J = 1 \leftarrow 0$ transition of OCS, assuming a dipole moment of 0.71519(3) D.[46]

Ab initio optimizations were performed using Gaussian 09[47] at the MP2/6-311++G(2d,2p) level with the CALCALL and VERYTIGHT options, and constrained to C_{6v} symmetry.

Results and Discussion

Ab Initio Calculations

Based on recent results for fluorobenzene···HCCH[18] and for other benzene complexes,[21-24, 48] it was assumed that the structure of BZ···HCCH would have C_{6v} or effective C_{6v} symmetry, with the HCCH oriented perpendicular to the center of the aromatic ring. An initial optimization at the MP2/6-311++G(2d,2p) level, assuming C_{6v} symmetry, provided an initial estimate of the rotational constants of the dimer (Table 1) and predicted a dipole moment of about 0.48 D, which is sufficiently large that the rotational spectrum should be readily observed using the UVa CP-FTMW spectrometer.

Spectra

The spectrum of a symmetric top with rotational constants consistent with ab initio predictions for BZ···HCCH was easily identified and assigned from the broadband scan (Figure 1). The observed intensities were consistent, at low K, with the expected 10:22:18:28:18:22:20 intensity ratio (for $K = 0 - 6$) in a C_{6v} symmetric top, with exchange of six equivalent hydrogen atoms;[49] however, at higher K, intensities dropped off much more rapidly than expected, likely due to low population of the higher K levels in the cold molecular expansion. The signal-to-noise ratio (S/N) of the most abundant isotopologue (~400 – 500 for the strongest transitions) was sufficient that the $^{13}C^{12}C_5H_6$···HCCH species was also observed and assigned from the

7

broadband scan (Figure 1, S/N ~20 – 30 for the strongest transitions). The intensity of the ^{13}C species was about 6% of the main isotopologue, consistent with all six benzene carbon atoms being equivalent in the dimer structure. The ^{13}C^{12}C$_5$H$_6$ isotopologue spectrum was that of a very near prolate asymmetric top ($\kappa = -0.9940$), as expected when the symmetry of the parent species is broken by isotopic substitution. In addition, a few transitions that appeared to be consistent with the two ^{12}C$_6$H$_6$···H^{13}C^{12}CH isotopologues (1% abundance) were identified in the broadband scan. These were confirmed and the assignment of these two additional ^{13}C species was completed using an enriched H^{13}C^{12}CH sample and the resonant cavity FTMW spectrometer at EIU. A second broadband scan performed at UVa using C$_6$H$_5$D led to assignment of the C$_6$H$_5$D···HCCH isotopologue. The S/N of this scan was not sufficient to observe ^{13}C substitutions on the benzene ring; since the deuterium breaks the symmetry of the parent species, the aromatic carbon atoms are no longer equivalent, leading to transitions too weak to observe. Unresolved splitting of the rotational transitions due to the quadrupolar deuterium nucleus leads to additional loss of intensity in these spectra. Spectroscopic constants for all isotopologues are reported in Table 1, and fitted transition frequencies are given in Tables 2 and 3. Asymmetric top isotopologues were fitted with an *S*-reduction Watson Hamiltonian in the I^r representation.[50]

In addition to the assigned spectrum, several sets of much weaker transitions were observed (Figure 1), falling to the low frequency side of the BZ···HCCH symmetric top lines. For each $J + 1 \leftarrow J$ level of the ground state spectrum, three clusters, each consisting of ~3 – 5 additional lines, spread over several megahertz, were observed (Table 4). Although the splitting patterns do not match those of a ground state symmetric top, the center frequencies of each cluster scale with J similarly to the ground state transitions. It is believed that these transitions belong to excited states of the low energy intermolecular vibrational modes of the dimer. These

would originate from two doubly degenerate "bending" modes and a singly degenerate stretching mode, corresponding to the two rotational and three translational degrees of freedom of free HCCH. Böning, *et al*[15] used dispersed fluorescence to determine intermolecular vibrational frequencies for BZ···HCCH of 62.4 cm^{-1}, 94 cm^{-1} and 131.7 cm^{-1}, for degenerate hindered rotation of HCCH relative to BZ, degenerate translation of HCCH relative to BZ, and non-degenerate translation of HCCH perpendicular to BZ, respectively; however, their results did not agree well with harmonic frequency calculations. In the present study, anharmonic frequency calculations aimed at aiding assignment and analysis of these excited state transitions have proven challenging. A future publication will further explore the theoretical prediction and analysis of this spectrum, as well as including a more detailed analysis of the excited state transitions.

Dipole moment

The dipole moment of BZ···HCCH was determined by fitting nineteen Stark shifted frequencies from four *M* components of three rotational transitions. Kisiel's QSTARK program[51] allows fitting and prediction of mixed first and second order Stark shifts, although only second order shifts (for $K = 0$ and/or $M = 0$ transitions) were fitted, since first order Stark shifts were too fast to measure reliably using the EIU resonant cavity FTMW instrument. The results are summarized in Table 5, with details of the fitted transitions provided as Electronic Supplementary Information. The fitted dipole moment is 0.438(11) D, in reasonable agreement with the MP2/6-311++G(2d,2p) value of 0.48 D. The minimal structural distortion of the two monomer subunits within the dimer in the MP2 calculation accounts only for ~0.02 D. The remainder of the dimer dipole moment must therefore be due to monomer electronic charge

redistribution. Further computational work exploring the dipoles induced in each monomer as they approach each other should yield insight into the charge rearrangement within the complex, although this is beyond the scope of the current work. The ab initio optimization of BZ···HCCH also indicates that the negative end of the dipole lies towards the acetylene molecule, likely arising from polarization of the BZ π electrons towards the slight positive charge of the acetylenic hydrogen atom. This is in agreement with the induced dipole observed in recent work on fluorobenzene···HCCH.[18] The ability of the relatively acidic HCCH to polarize the BZ electrons is confirmed by noting that the dipole moments of BZ···Ar and BZ···Kr are considerably smaller (0.12(4) D[52] and 0.136(2) D[53], respectively), although the direction of these induced dipoles is not known.

Structure

The structure of the BZ···HCCH dimer has been determined using both Kraitchman's single substitution equations via the KRA program[54, 55,] (assuming C_{6v} symmetry), and with an inertial fit via the STRFITQ program.[56] For the inertial fit, the structure was determined first assuming C_{6v} symmetry, and then again by allowing the HCCH, BZ, or both to tip slightly away from the C_6 axis of BZ (Figure 2). The resulting structural parameters are summarized in Table 6, and a comparison of principal axis coordinates from the different fits is shown in Table 7. Monomer structures were assumed to be unchanged from literature values and are given for reference in Table 8.[57, 58] In all tabulated r_0 structures, only I_b from the five isotopic species was fitted. Fits that additionally included I_a for asymmetric top isotopologues, were also attempted, and these gave consistent structural parameters but had large uncertainties due to the poorly determined A rotational constants (Table 1). Finally, assuming a C_{6v} structure, it was also

possible to calculate the intermolecular distance using I_b from each isotopologue individually. Although not included in Table 6, these R_{cm} distances range from 4.1542 Å – 4.1548 Å, in excellent agreement with the least-squares fits. Although the fit that allows both acetylene and benzene to tilt relative to the symmetry axis has the lowest standard deviation, that is also a fit of five moments of inertia to three structural parameters and, thus, is not as over-determined as the other structure fits that were attempted, possibly giving an artificially low uncertainty, and also showing indications that the fitted angles may not be totally independent. In addition, the uncertainties in the fitted angles are of similar order of magnitude to the angles themselves. The center-of-mass (R_{cm}) and H$\cdots\pi$ distances derived from the C_{6v} structure and from the structure where both monomers are allowed to tip agree to within the experimental uncertainties; thus, the C_{6v} structure will be used for comparison with other species (see below), since the observed spectrum was that of a symmetric top, indicating effective C_{6v} symmetry. This does not preclude the likelihood that the two subunits oscillate around the equilibrium structure with small nonzero angles; however, these angles are not accurately determinable from the experimental data. The likely existence of low energy intermolecular vibrations is further confirmed by the multiple excited state spectra that have been observed (see Spectra section, above).

Kraitchman substitution coordinates (Table 7) were also obtained for the three unique carbon atoms (assuming a symmetric top) and one hydrogen atom on the benzene ring. These coordinates agree very well with the principal axis coordinates derived from the various inertial fits. The r_s intermolecular parameters are included in Table 6 for comparison with the r_0 values. The substitution parameters are slightly smaller than the values from the inertial fit, consistent with the fact that substitution parameters typically lie between average and equilibrium values.[59] In addition, a tilt angle for HCCH may be derived by assuming that the monomer is unchanged

from the literature structure,[57] and that the C-C distance derived from the r_s coordinates is actually a projection of the C≡C bond onto the *a*-axis. This gives a tilt (θ, Figure 2) of about 4.9º from an axis connecting the centers of mass of the two monomers. For benzene, the tilt of the benzene plane away from a line perpendicular to the axis connecting the centers of mass of the two monomers may be estimated from the difference in hydrogen and carbon r_s *a*-coordinates, again with the assumption that the monomer structure is unchanged from the literature value.[58] This gives an angle (ϕ, Figure 2) of about 1.3º. Both of these results are in reasonable agreement with inertial fits, which indicate an acetylene tilt of 5 − 7º and a benzene tilt of less than 1º (Table 6).

Finally, the BZ monomer structure and the C≡C distance of HCCH monomer may be calculated from the r_s coordinates. This gives an HCCH C≡C distance of 1.1986(7) Å, BZ C$\cdots$C distance of 1.4043(12) Å, and BZ C–H distance of 1.0853(12) Å. These are all in reasonable agreement with literature values (Table 8).

Binding Energy and Comparison with Related Species

The intermolecular stretching force constant and the binding energy of the dimer may be estimated assuming a pseudo-diatomic approximation and a Lennard-Jones potential, as shown in equations (1) and (2).[60, 61] Although the absolute values of these binding energies may differ by several kJ mol^{-1} from experimental values determined by other methods, comparisons to values for related complexes determined using a similar approach should reasonably well reproduce trends in binding energy.

$$k_s = \frac{16\pi^4 (\mu R_{cm})^2 [8B^4]}{hD_J}$$

(1)

$$E_B = \frac{1}{72} k_s R_{cm}^2$$

(2)

These give $k_s = 4.9(5)$ N m^{-1} and $E_B = 7.1(7)$ kJ mol^{-1}. This binding energy is in the middle of

the range (~6 − 9 kJ mol^{-1}) observed for other benzene complexes having effective C_{6v} symmetry

and XH···π interactions (see Table 9), although the force constant is significantly smaller than

observed for those complexes. In addition, the majority of previously studied benzene

complexes (with more acidic partners) have XH···π distances of ~2.35 − 2.38 Å,[13, 14, 21-24] while

the observed distance for BZ···HCCH is significantly longer, at 2.4921(1) Å. The pK_a values of

HCCH (p$K_a = 25$)[28] and HCF$_3$ (p$K_a = 25.5$)[31] are nearly identical; hence, the closest comparison

should be made between these two prototypical activated CH···π complexes. Again, it is

interesting to note that E_B is similar for the two systems (7.1(7) kJ mol^{-1} for BZ···HCCH vs. 8.4

kJ mol^{-1} for BZ···HCF$_3$), but the CH···π distance is significantly longer in the HCCH complex

(2.4921(1) Å in BZ···HCCH vs. 2.366(2) Å in BZ···HCF$_3$). This lengthening is consistent with

the smaller force constant also observed for BZ···HCCH. It is possible that the increased length

in BZ···HCCH is due to the different nature of the electrostatic interactions in that complex,

which must be driven by quadrupole-quadrupole interactions between BZ and HCCH, while in

BZ···HCF$_3$ existence of dipole-quadrupole interactions may draw the two monomers closer

together. The balance between smaller k_s and larger R_{cm} in BZ···HCCH leads to the similar

estimates of binding energy for the two dimers. A separate study by Shibasaki, *et al.*[11] gave a

slightly higher binding energy of 11.3(8) kJ mol^{-1} for BZ···HCCH; however, this is not directly

comparable to the estimate made in the current work, due to the different approximations

required for the present result. Calculations by Tsuzuki give an interaction energy for

BZ···HCCH that is about 68% of the value for BZ···HCF$_3$, roughly consistent with the present

experimental results.[62] Tsuzuki's value is broken down into electrostatic, repulsive and

dispersion terms which indicate that, although the electrostatic interaction is similar in the two

complexes, the dispersion interaction is significantly stronger in the HCF_3 complex, consistent

with the fact that HCF_3 is considerably more electron rich than HCCH.[62] This could be a cause

both for the shorter CH$\cdots\pi$ distance and the higher binding energy of BZ$\cdots HCF_3$.

Finally, comparison may also be made between BZ$\cdots$HCCH and

fluorobenzene$\cdots$HCCH.[18] In the latter complex, the force constant ($k_s = 2.8(6)$ N m^{-1}) and

binding energy (4.1(8) kJ mol^{-1}) are both significantly smaller than in BZ$\cdots$HCCH. This is

likely due to the electrostatic effects of ring fluorination, as discussed in ref. 18. On the other

hand, the observed CH$\cdots\pi$ distance is nearly identical in the two complexes. This again points to

the intermolecular distance being determined by the fact that the binding partner with the

aromatic molecule is nonpolar, and is also consistent with the similar observed distance in BZ

dimer.[16, 17] It would be interesting to pursue investigations of difluorobenzenes with HCCH to

further evaluate the effects of ring fluorination on CH$\cdots\pi$ interactions, and experimental and

theoretical studies of *o*-difluorobenzene$\cdots$HCCH are currently in progress.[63]

Conclusions

High resolution FTMW spectroscopy experiments have confirmed that the prototype

CH$\cdots\pi$ complex BZ$\cdots$HCCH has effective C_{6v} symmetry, with the HCCH axis lying nearly

perpendicular to the plane of the aromatic ring. This complex provides an example of an

activated CH$\cdots\pi$ interaction, similar to that observed by López in BZ$\cdots HCF_3$ (where the two

proton donors have similar acidities). The acidic nature of acetylene is indicated by the

relatively large induced dipole in BZ$\cdots$HCCH of 0.438(11) D. Both r_0 and r_s structure

3/20/2014 10:13:21 AM

determinations suggest that at equilibrium there is likely a tilt of about 5° of the HCCH axis away from the BZ C_6 axis, although the large uncertainty in this angle prevents its accurate determination. This is consistent with previously observed structures of other complexes of BZ with strong and weak acids (HX, with X = F,[23] Cl,[22] Br,[21] CN,[24] CF$_3$[13, 14]) and linear molecules (such as OCS[48]).

The observed binding energy for BZ···HCCH is similar to those determined by the same method for other BZ···HX complexes; however, the H···π distance is significantly longer than for any of the previously studied species. In addition, the observed H···π distance is longer than the BZ···HCCH cocrystal.[40] The differences could partially be a result of low frequency vibrational motions within the gas phase complex, leading to the observation of an average structure. In addition, the crystal packing is likely to constrain the structure somewhat. Evidence of structural averaging comes from the observation of a symmetric top spectrum despite the fact that the observed rotational constants are more consistent with a structure in which HCCH tilts slightly away from the symmetry axis of BZ. Also, observation of three additional sets of weaker transitions, corresponding to slightly smaller rotational constants, but following roughly a symmetric top or near symmetric top spacing between adjacent *J* values, appears to be consistent with low energy intermolecular vibrational modes of the dimer. These unique excited state spectra will be analyzed in detail in a future publication.

Tables

Table 1. Experimental and ab initio spectroscopic constants for BZ⋯HCCH, including the four isotopically substituted species.

	Ab Initio [a]	C_6H_6⋯HCCH	C_6H_6⋯$H^{13}C^{12}CH$ [b]	C_6H_6⋯$H^{12}C^{13}CH$ [c]	$^{13}C^{12}C_5H_6$⋯HCCH	C_6H_5D⋯HCCH
A / MHz	2846	–	–	–	2837(13)	2764.1(7)
B / MHz	1199	1148.89656(25)	1132.7251(4)	1114.2052(3)	1146.1883(4)	1146.2664(3)
C / MHz	1199	–	–	–	1141.1364(4)	1130.4918(3)
D_J / kHz	–	1.207(3)	1.200(7)	1.151(6)	1.194(5)	1.179(3)
D_{JK} / kHz	–	19.977(11)	19.36(4)	19.36(3)	19.81(4)	19.347(12)
RMS / kHz [d]	–	2.2	1.8	1.4	3.7	6.0
N [e]	–	22	13	15	21	25

[a] For the parent species.
[b] ^{13}C closest to the benzene ring.
[c] ^{13}C furthest from the benzene ring.
[d] $RMS = \left(\frac{\Sigma (v_{obs} - v_{calc})^2}{N} \right)^{\frac{1}{2}}$
[e] N = number of transitions in fit.

Table 2. Fitted transition frequencies for the normal and symmetric top isotopologues of BZ···HCCH. All frequencies are in MHz.

				"Normal"		$C_6H_6···H^{13}C^{12}CH$ [a]		$C_6H_6···H^{12}C^{13}CH$ [b]	
J'	K'	J''	K''	$v_{observed}$	Δv [c]	$v_{observed}$	Δv	$v_{observed}$	Δv
3	2	2	2	6892.7673	-0.0022	–	–	6684.6391	-0.0032
3	1	2	1	6893.1278	-0.0013	6796.1074	0.0023	6684.9912	0.0004
3	0	2	0	–	–	6796.2209	-0.0004	6685.1088	0.0019
4	3	3	3	9189.4248	-0.0004	9060.0970	-0.0034	8911.9522	-0.0008
4	2	3	2	9190.2261	0.0018	9060.8764	0.0018	8912.7296	0.0022
4	1	3	1	9190.7057	0.0020	9061.3389	-0.0002	8913.1923	0.0002
4	0	3	0	9190.8614	-0.0022	9061.4936	-0.0004	8913.3461	-0.0009
5	4	4	4	11485.1672	0.0013	–	–	–	–
5	3	4	3	11486.5656	0.0013	11324.9096	0.0000	11139.7325	-0.0015
5	2	4	2	11487.5649	0.0017	11325.8792	0.0019	11140.7026	0.0006
5	1	4	1	11488.1638	0.0013	11326.4573	-0.0007	11141.2834	0.0006
5	0	4	0	11488.3628	0.0005	11326.6508	-0.0007	11141.4768	0.0004
6	5	5	5	13779.7179	-0.0052	–	–	–	–
6	4	5	4	13781.8821	0.0015	–	–	–	–
6	3	5	3	13783.5568	-0.0018	–	–	13367.3779	0.0011
6	2	5	2	13784.7565	-0.0008	13590.7379	0.0019	13368.5391	0.0007
6	1	5	1	13785.4767	0.0002	13591.4343	0.0015	13369.2356	0.0002
6	0	5	0	13785.7163	0.0001	13591.6619	-0.0032	13369.4656	-0.0022
7	4	6	4	16078.4250	0.0035	–	–	–	–
7	3	6	3	16080.3835	0.0043	–	–	–	–

7	2	6	2	16081.7742	-0.0034	–	–	–	–
7	1	6	1	16082.6154	-0.0012	–	–	–	–
7	0	6	0	16082.8947	-0.0016	–	–	–	–

^{a} ^{13}C closest to the benzene ring.
^{b}^{13}C furthest from the benzene ring.
^{c} Observed minus calculated transition frequency.

Table 3. Fitted transition frequencies for asymmetric top isotopologues of BZ···HCCH. All frequencies are in MHz.

J'	K_a'	K_c'	J''	K_a''	K_c''	$\nu_{observed}$ ($^{13}C^{12}C_5H_6$···HCCH)	$\Delta\nu^a$	$\nu_{observed}$ (C$_6$H$_5$D···HCCH)	$\Delta\nu$
3	1	3	2	1	2	6854.1393	-0.0023	6806.2903	-0.0073
3	0	3	2	0	2	6861.7986	-0.0015	6829.6897	0.0019
3	1	2	2	1	1	6869.2979	0.0007	6853.6249	0.0041
4	1	4	3	1	3	9138.7070	-0.0016	9074.7912	-0.0074
4	3	1	3	3	0	9147.5966	0.0068	–	–
4	2	3	3	2	2	9148.3513	0.0007	9106.0193	-0.0029
4	2	2	3	2	1	9148.4701	0.0064	9107.1700	-0.0001
4	0	4	3	0	3	9148.8783	-0.0019	9105.5801	-0.0026
4	1	3	3	1	2	9158.9136	-0.0022	9137.8993	0.0056
5	1	5	4	1	4	11423.1479	-0.0018	11343.0693	-0.0048
5	4	1	4	4	0	–	–	11380.3648	0.0041
5	3	2	4	3	1	11434.2786	-0.0045	–	–
5	2	4	4	2	3	11435.2152	0.0060	11382.1725	0.0006
5	2	3	4	2	2	11435.4339	-0.0016	11384.4662	-0.0007
5	0	5	4	0	4	11435.7961	-0.0044	11380.9074	0.0015
5	1	4	4	1	3	11448.4077	-0.0009	11421.9426	0.0067
6	1	6	5	1	5	13707.4388	0.0052	13611.0676	-0.0019
6	5	1	5	5	0	–	–	13654.0081	-0.0048
6	4	2	5	4	1	–	–	13656.2090	0.0032
6	3	3	5	3	2	13720.8352	-0.0052	–	–

6	2	5	5	2	4	13721.9194	0.0042	–	–
6	2	4	5	2	3	13722.3078	-0.0034	13662.0961	-0.0018
6	0	6	5	0	5	13722.5190	-0.0020	13655.5180	0.0019
6	1	5	5	1	4	13737.7472	0.0034	13705.6943	0.0066
7	1	7	6	1	6	–	–	15878.7439	0.0122
7	0	7	6	0	6	–	–	15929.2680	-0.0066
7	2	6	6	2	5	–	–	15933.7219	0.0101
7	2	5	6	2	4	–	–	15940.1223	-0.0035
7	1	6	6	1	5	–	–	15989.0723	-0.0155

[a] Observed minus calculated transition frequency.

Table 4. Approximate frequencies for excited state transitions of BZ⋯HCCH (MHz). Tabulated frequencies correspond to the approximate center of each group of lines. See Figure 1 for an example of the full $J = 4 \leftarrow 3$ region of the spectrum.

$J' \leftarrow J''$	Ground State $(K = 0)$	Excited State 1	Excited State 2	Excited State 3
$3 \leftarrow 2$	6893.3	6599	6437	6273
$4 \leftarrow 3$	9190.9	8809	8577	8367
$5 \leftarrow 4$	11488.3	11012	10712	10451
$6 \leftarrow 5$	13785.8	13214	12840	12534
$7 \leftarrow 6$	16083.0	15412	14961	14616

Table 5. Stark effect data for BZ$\cdots$HCCH.[a]

$J_K' \leftarrow J_K''$	$\lvert M \rvert$	Number of electric fields
$3_0 \leftarrow 2_0$	1	6
	2	3
$3_1 \leftarrow 2_1$	0	6
$4_0 \leftarrow 3_0$	3	4
	RMS:	5.8 kHz
	μ:	0.438(11) D

[a] The full list of measured transition frequencies for the Stark effects at each electric field value is available as Electronic Supplementary Information.

Table 6. Derived and fitted structural parameters for BZ$\cdots$HCCH, allowing different combinations of parameters to vary (see Figure 2 for angle definitions). For r_0 structures, I_b only was fitted from all five isotopologues. See text for discussion.

	r_0 (R_{cm})[a]	r_0 (R_{cm}, θ)	r_0 (R_{cm}, ϕ)	r_0 (R_{cm}, θ, ϕ)	r_s	Ab Initio[b]
R_{cm} / Å	4.1546(1)	4.1560(8)	4.1547(1)	4.1554(5)	4.1320(15)	4.0387
θ / °	–	7.4(2.2)	–	5.6(1.9)	–	
ϕ / °	–	–	1.0(4)	0.8(2)	–	
$R_{CH\cdots\pi}$ / Å[c]	2.4921(1)	2.5073(14)	2.4922(1)	2.5008(89)	2.4717(7)[d]	2.3694
σ / u Å^2 [e]	0.038	0.025	0.017	0.015	–	

[a] Assuming C_{6v} symmetry.
[b] MP2/6-311++G(2d,2p).
[c] Perpendicular distance from H atom to the benzene plane (derived from fitted parameters R_{cm}, θ, and ϕ).
[d] Derived assuming acetylenic C–H distance equal to literature value of 1.061 Å.
[e] Standard deviation of fitted moments of inertia.

Table 7. Principal axis coordinates (Å) for r_s structure, as well as r_0 structures either constrained to C_{6v} symmetry, or allowing both θ and ϕ to vary (see Figure 2 for angle definitions).[a] Ab initio principal axis coordinates (r_e) are included for comparison. Full sets of principal axis coordinates for the r_e and all r_0 structures are available as Electronic Supplementary Information.

C nearest to BZ	a-coordinate	b-coordinate
$\|r_s\|$	2.5138(6)	0
r_0 (C_{6v})	–2.5144	0
r_0 (angles varied, C_s)	–2.5179	–0.0596
r_e (C_{6v})	–2.4225	0
C farthest from BZ		
$\|r_s\|$	3.7124(4)	0
r_0 (C_{6v})	–3.7174	0
r_0 (angles varied, C_s)	–3.7152	0.0575
r_e (C_{6v})	–3.6352	0
C on BZ		
$\|r_s\|$	1.0189(15)	1.4043(11)
r_0 (C_{6v})	1.0386	±1.3969
r_0 (angles varied, C_s)[b]	1.0190, 1.0587	–1.3963, 1.3971
r_e (C_{6v})	1.0099	±1.3967
H on BZ		
$\|r_s\|$	0.9945(15)	2.4893(6)
r_0 (C_{6v})	1.0386	±2.4784
r_0 (angles varied, C_s)[b]	1.0036, 1.0741	–2.4777, 2.4785
r_e (C_{6v})	1.0059	±2.4775

[a] Reported uncertainties in r_s coordinates are the Costain errors, as implemented in the KRA program.[54, 55] Based on observed uncertainties in the structural parameters reported in Table 6, maximum uncertainties in r_0 coordinates are estimated to be ±0.0002 Å for the C_{6v} structure and ±0.010 Å for the structure where angles were varied.

[b] When HCCH and BZ are allowed to tip away from the BZ C_6 axis, the BZ carbon and hydrogen atoms lying along the positive and negative *b*-axis are no longer equivalent; thus, the first set of coordinates given corresponds to the BZ carbon atom nearest to the HCCH H atom, and the second set of coordinates corresponds to the BZ carbon atom that is tipped away from HCCH.

Table 8. Literature structures for HCCH[57] and BZ[58] monomers.

	HCCH	BZ
R_{C-C} / Å	1.203	1.3969
R_{C-H} / Å	1.061	1.0815

Table 9. Force constants and binding energies for XH···π benzene complexes.

	k_s / N m^{-1} [a]	E_B / kJ mol^{-1} [a]	H···π distance / Å [b]
BZ···HF[23]	7.3	6.0	2.25(2)
BZ···HCl[22]	8.0	8.6	2.35(2)
BZ···HBr[21]	7.65	9.1	2.36(2)
BZ···HCF$_3$[13, 14]	6.8	8.4	2.366(2)
BZ···HCN[24]	6.6	8.9	2.38(2)
BZ···HCCH [c]	4.9(5)	7.1(7)	2.4921(1)

[a] k_s and E_B values based on approximations, as described in eqn. (1) and (2) in the text.
[b] Perpendicular distance from the H atom to the ring plane.
[c] This work.

Figure Captions

Figure 1. The $J = 4 \leftarrow 3$ region of the broadband spectrum of BZ···HCCH. The ground state (red) corresponds to the transitions around 9190 MHz, the $^{13}CC_5H_6$ isotopologue (green) is around 9150 MHz, and the remaining three clusters of lines to lower frequency (blue) are excited states.

Figure 2. Structural definition for BZ···HCCH. The average structure has C_{6v} symmetry – see text.
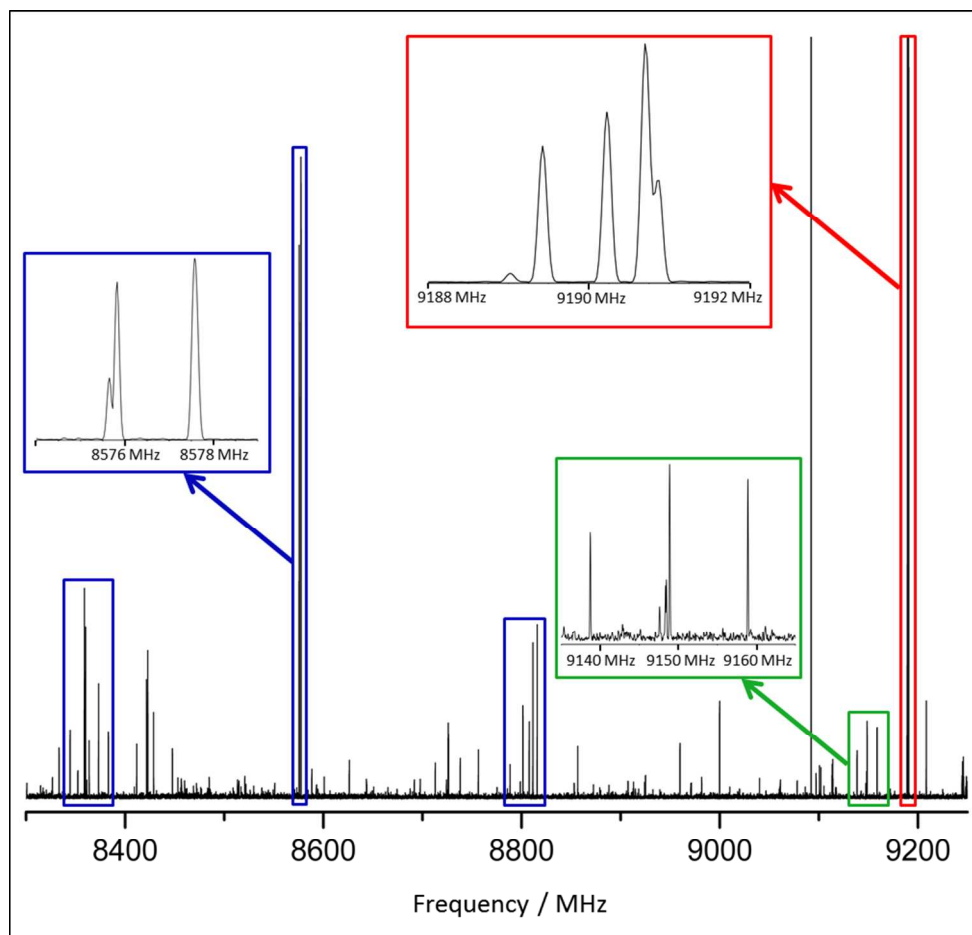
Figures

Figure 1.

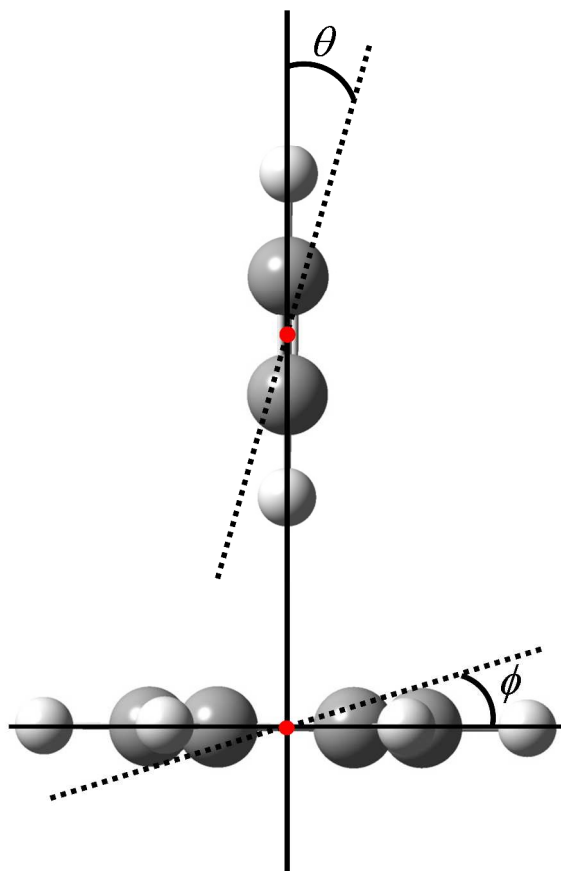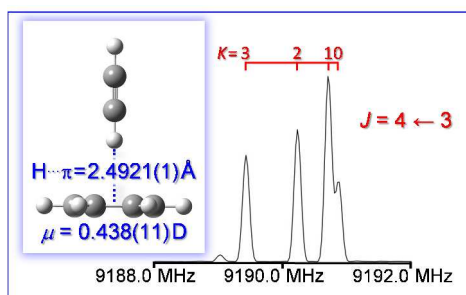**Figure 2.**

Graphical Table of Contents Entry

The benzene···acetylene dimer is a symmetric top with $\mu = 0.438(11)$ D and H···π = 2.4921(1) Å.

References

[1] M. Tamres, *J. Am. Chem. Soc.*, 1952, **74**, 3375.

[2] M. Nishio, M. Hirota, Y. Umezawa, *The CH/π Interaction: Evidence, Nature, and Consequences*, Wiley-VCH, New York, 1998, and references therein.

[3] M. Nishio, *The CH/π Interaction: A weak hydrogen-bond occurring between soft acids and soft bases*, http://www.tim.hi-ho.ne.jp/dionisio/, accessed 1/20/14.

[4] O. Takahashi, Y. Kohno, S. Iwasaki, K. Saito, M. Iwaoka, S. Tomoda, Y. Umezawa, S. Tsuboyama, M. Nishio, *Bull. Chem. Soc. Jap.*, 2001, **74**, 2421.

[5] E. Carrasquillo M., T. S. Zwier, D. H. Levy, *J. Chem. Phys.*, 1985, **83**, 4990.

[6] J. R. Gord, A. W. Garrett, R. E. Bandy, T. S. Zwier, *Chem. Phys. Lett.*, 1990, **171**, 443.

[7] B. Reimann, K. Buchhold, S. Vaupel, B. Brutschy, Z. Havlas, V. Špirko, P. Hobza, *J. Phys. Chem. A*, 2001, **105**, 5560.

[8] A. Fujii, S. Morita, M. Miyazaki, T. Ebata, N. Mikami, *J. Phys. Chem. A*, 2004, **108**, 2652.

[9] S. Morita, A. Fujii, N. Mikami, S. Tsuzuki, *J. Phys. Chem. A*, 2006, **110**, 10583.

[10] K. Shibasaki, A. Fujii, N. Mikami, S. Tsuzuki, *J. Phys. Chem. A*, 2006, **110**, 4397.

[11] K. Shibasaki, A. Fujii, N. Mikami, S. Tsuzuki, *J. Phys. Chem. A*, 2007, **111**, 753.

[12] S. Chervenkov, P. Wang, J. E. Braun, T. Chakraborty, H. J. Neusser, *Phys. Chem. Chem. Phys.*, 2007, **9**, 837.

[13] J. C. López, W. Caminati, J. L. Alonso, *Angew. Chem. Int. Ed. Eng.*, 2006, **45**, 290 –293.

[14] Q. Gou, G. Feng, L. Evangelisti, D. Loru, J. L. Alonso, J. C. López, W. Caminati, *J. Phys. Chem. A*, 2013, **117**, 13531.

[15] M. Böning, B. Stuhlmann, G. Engler, M. Busker, T. Häber, A. Tekin, G. Jansen, K. Kleinermanns, *ChemPhysChem*, 2013, **14**, 837.

[16] E. Arunan, H. S. Gutowsky, *J. Chem. Phys.*, 1993, **98**, 4294.

[17] M. Schnell, U. Erlekam, P. R. Bunker, G. von Helden, J.-U. Grabow, G. Meijer, A. van der Avoird, *Angew. Chem. Int. Ed.*, 2013, **52**, 1.

[18] N. W. Ulrich, T. S. Songer, R. A. Peebles, S. A. Peebles, N. A. Seifert, C. Pérez, B. P. Pate, *Phys. Chem. Chem. Phys.*, 2013, **15**, 18148.

[19] M. Busker, T. Häber, M. Nispel, K. Kleinermanns, *Angew. Chem. Int. Ed. Eng.*, 2008, **47**, 10094.

[20] S. Tsuzuki, *Annu. Rep. Prog. Chem., Sect. C: Phys. Chem.*, 2012, **108**, 69.

[21] S. A. Cooke, C. K. Corlett, C. M. Evans, A. C. Legon, *Chem. Phys. Lett.*, 1997, **272**, 61.

[22] W. G. Read, E. J. Campbell, G. Henderson, *J. Chem. Phys.*, 1983, **78**, 3501.

[23] F. A. Baiocchi, J. H. Williams and W. Klemperer, *J. Phys. Chem.*, 1983, **87**, 2079.

[24] H. S. Gutowsky, E. Arunan, T. Emilsson, S. L. Tschopp, C. E. Dykstra, *J. Chem. Phys.*, 1995, **103**, 3917.

[25] A. Arunan, T. Emilsson, H. S. Gutowsky, G. T. Fraser, G. de Oliveira, C. E. Dykstra, *J. Chem. Phys.*, 2002, **117**, 9766.

[26] S. Suzuki, P. G. Green, R. E. Bumgarner, S. Dasgupta, W. A. Goddard, III, G. A. Blake, *Science*, 1992, **257**, 942.

[27] H. S. Gutowsky, T. Emilsson, E. Arunan, *J. Chem. Phys.*, 1993, **99**, 4883.

[28] M. Jones, Jr., *Organic Chemistry 2nd Edition*, W. W. Norton and Co., New York, 2000.

[29] Th. Brupbacher, J. Makarewicz, A. Bauder, *J. Chem. Phys.*, 1994, **101**, 9736.

[30] A. Fujii, K. Shibasaki, T. Kazama, R. Itaya, N. Mikami, S. Tsuzuki, *Phys. Chem. Chem. Phys.*, 2008, **10**, 2836.

[31] K. I. Butin, A. N. Kashin, I. P. Beletskaya, L. S. German, V. R. Polishchuk, *J. Organomet. Chem.*, 1970, **25**, 11.

[32] S. Tsuzuki, K. Honda, T. Uchimaru, K. Tanabe, *J. Am. Chem. Soc.*, 2000, **122**, 3746.

[33] S. Tsuzuki, K. Honda, T. Uchimaru, M. Mikami, J. Tanabe, *J. Phys. Chem. A*, 2002, **106**, 4423.

[34] K. Sundararajan, K. S. Viswanathan, A. D. Kulkarni, S. R. Gadre, *J. Mol. Struct.*, 2002, **613**, 209.

[35] A. Tekin, G. Jansen, *Phys. Chem. Chem. Phys.*, 2007, **9**, 1680.

[36] M. Majumder, B. K. Mishra, N. Sathyamurthy, *Chem. Phys. Lett.*, 2013, **557**, 59.

[37] B. K. Mishra, S. Karthikeyan, V. Ramanathan, *J. Chem. Theory Comp.*, 2012, **8**, 1935.

[38] P. Jantimapornkij, P. Jundee, N. Uttamapinant, S. Pianwanit, A. Karpfen, *Comp. and Theor. Chem.*, 2012, **999**, 231.

[39] T. C. Dinadayalane, G. Paytakov, J. Leszczynsky, *J. Mol. Model*, 2013, **19**, 2855.

[40] R. Boese, T. Clark, A. Gavizzotti, *Helv. Chim. Acta*, 2003, **86**, 1085.

[41] F. Meyer-Wegner, H. W. Lerner, M. Bolte, *Acta Cryst. C*, 2010, **66**, o182.

[42] G. G. Brown, B. C. Dian, K. O. Douglass, S. M. Geyer, S. T. Shipman, B. H. Pate, *Rev. Sci. Inst.*, 2008, **79**, 053103.

[43] C. Pérez, S. Lobsiger, N. A. Seifert, D. P. Zaleski, B. Temelso, G. C. Shields, Z. Kisiel, B. H. Pate, *Chem. Phys. Lett.* 2013, **571**, 1.

[44] J. J. Newby, M. M. Serafin, R. A. Peebles, S. A. Peebles, *Phys. Chem. Chem. Phys.*, 2005, **7**, 487.

[45] T. J. Balle, W. H. Flygare, *Rev. Sci. Instrum.*, 1981, **52**, 33.

[46] J. M. L. J. Reinartz, A. Dymanus, *Chem. Phys. Lett.*, 1974, **24**, 346.

[47] Gaussian 09, Revision C.01, M. J. Frisch, G. W. Trucks, H. B. Schlegel, G. E. Scuseria, M. A. Robb, J. R. Cheeseman, G. Scalmani, V. Barone, B. Mennucci, G. A. Petersson, H. Nakatsuji, M. Caricato, X. Li, H. P. Hratchian, A. F. Izmaylov, J. Bloino, G. Zheng, J. L. Sonnenberg, M. Hada, M. Ehara, K. Toyota, R. Fukuda, J. Hasegawa, M. Ishida, T. Nakajima, Y. Honda, O. Kitao, H. Nakai, T. Vreven, J. A. Montgomery, Jr., J. E. Peralta, F. Ogliaro, M. Bearpark, J. J. Heyd, E. Brothers, K. N. Kudin, V. N. Staroverov, T. Keith, R. Kobayashi, J. Normand, K. Raghavachari, A. Rendell, J. C. Burant, S. S. Iyengar, J. Tomasi, M. Cossi, N. Rega, J. M. Millam, M. Klene, J. E. Knox, J. B. Cross, V. Bakken, C. Adamo, J. Jaramillo, R. Gomperts, R. E. Stratmann, O. Yazyev, A. J. Austin, R. Cammi, C. Pomelli, J. W. Ochterski, R. L. Martin, K. Morokuma, V. G. Zakrzewski, G. A. Voth, P. Salvador, J. J. Dannenberg, S. Dapprich, A. D. Daniels, O. Farkas, J. B. Foresman, J. V. Ortiz, J. Cioslowski, and D. J. Fox, Gaussian, Inc., Wallingford CT, 2010.

[48] U. Dahmen, H. Dreizler, W. Stahl, *Ber. Bunsenges. Phys. Chem.*, 1995, **99**, 434.

[49] Th. Brupbacher, A. Bauder, *J. Chem. Phys.*, 1993, **99**, 9394.

[50] J. K. G. Watson in *Vibrational Spectra and Structure, Vol. 6*; J. R. Durig, Ed., Elsevier, New York, 1977.

[51] Z. Kisiel, J. Kosarzewski, B.A. Pietrewicz, L. Pszczółkowski, *Chem. Phys. Lett.*, 2000, **325**, 523.

[52] Th. Brupbacher, A. Bauder, *Chem. Phys. Lett.*, 1990, **173**, 435.

[53] T. D. Klots, T. Emilsson, H. S. Gutowsky, *J. Chem. Phys.*, 1992, **97**, 5335.

[54] J. Kraitchman, *Am. J. Phys.*, 1953, **21**, 17.

[55] Kraitchman coordinates and structures from the KRA and EVAL code, Z. Kisiel, PROSPE–Programs for Rotational Spectroscopy; http://info.ifpan.edu.pl/~kisiel/prospe.htm

[56] R. H. Schwendeman in *Critical Evaluation of Chemical and Physical Structural Information*; D. R. Lide, M. A. Paul, Eds., National Academy of Sciences, Washington, DC, 1974. The STRFITQ program used in this work is the University of Michigan modified version of Schwendeman's original code.

[57] M. D. Harmony, V. W. Laurie, R. L. Kuczkowski, R. H. Schwendeman, D. A. Ramsay, F. J. Lovas, W. J. Lafferty, A. G. Maki, *J. Phys. Chem. Ref. Data*, 1979, **8**, 619.

[58] J. Pliva, J. W. C. Johns, L. Goodman, *J. Mol. Spectrosc.*, 1990, **140**, 214.

[59] W. Gordy, R. L. Cook, *Microwave Molecular Spectra, 3rd Ed.*, John Wiley and Sons, New York, 1984.

[60] D. J. Millen, *Can. J. Chem.,* 1985, **63**, 1477.

[61] T. J. Balle, E. J. Campbell, M. R. Keenan, W. H. Flygare, *J. Chem. Phys*., 1980, **72**, 922.

[62] S. Tsuzuki, K. Honda, T. Uchimaru, M. Mikami, A. Fujii, *J. Phys. Chem. A*, 2006, **110**, 10163.

[63] A. G. Akmeemana, R. A. Peebles, S. A. Peebles, B. H. Pate, N. A. Seifert, in progress, 2014.